



# The formation mechanism of corrosion scale and electrochemical characteristic of low alloy steel in carbon dioxide-saturated solution

J.B. Sun<sup>a,\*</sup>, G.A. Zhang<sup>b</sup>, W. Liu<sup>c</sup>, M.X. Lu<sup>c</sup>

<sup>a</sup> School of Mechanical and Electronic Engineering, China University of Petroleum, 739 Beiyi Road, Dongying 257061, PR China

<sup>b</sup> School of Chemistry and Chemical Engineering, Huazhong University of Science and Technology, Hubei Key Laboratory of Materials Chemistry and Service Failure, Wuhan 430074, PR China

<sup>c</sup> School of Materials Science and Engineering, University of Science and Technology Beijing, 30 Xueyuan Road, Beijing 100083, PR China

## ARTICLE INFO

### Article history:

Received 13 September 2011

Accepted 26 December 2011

Available online 2 January 2012

### Keywords:

A. Steel

B. EIS

B. SEM

C. Acid corrosion

## ABSTRACT

The formation mechanism of corrosion scale and electrochemical characteristic of low alloy steel in CO<sub>2</sub>-saturated solution were investigated by electrochemical measurements and surface characterization. The results show that the electrochemical behavior is associated with the formation of corrosion scale and the microstructure of steel. At the initial polarization stage, ferrite dissolves preferentially and leaves Fe<sub>3</sub>C behind, which results in high Fe<sup>2+</sup> ions concentration between lamellar Fe<sub>3</sub>C. This situation facilitates the formation of FeCO<sub>3</sub> scale between the lamellar Fe<sub>3</sub>C. With further increase of polarization times, the whole electrode surface is covered by FeCO<sub>3</sub> scale.

Crown Copyright © 2011 Published by Elsevier Ltd. All rights reserved.

## 1. Introduction

It is acknowledged that CO<sub>2</sub> corrosion would cause the failure of pipelines and equipments and result in great economic loss and catastrophic accidents. In addition, the leakage of crude oil due to CO<sub>2</sub> corrosion would induce fire accident, pollution of water resource and environment. Therefore, CO<sub>2</sub> corrosion has been one of the most common corrosion problems in oil and gas industry due to the high general corrosion rate and severe localized corrosion [1–4].

Although CO<sub>2</sub> corrosion had been extensively studied to understand its mechanism and to minimize the corrosion rate of steel and many models had been presented for the prediction of CO<sub>2</sub> corrosion [5–9], the mechanism of CO<sub>2</sub> corrosion is still not well understood since CO<sub>2</sub> corrosion is correspondingly complicated, with a number of factors affecting the corrosion process of steel. Many investigations [10–13] had demonstrated that the microstructure of steel plays an important role in the corrosion in CO<sub>2</sub>-containing environment, although there is no agreement on this issue. Most investigators suggested that carbon steels with ferritic–pearlitic microstructure exhibit better corrosion resistance than those with martensitic or bainitic microstructure [14–16]. However, there are also some investigators holding the opposite views [17–21]. The former claimed that the protective corrosion scales formed easily on the steel with ferritic–pearlitic microstructure in CO<sub>2</sub>-containing solution, which can improve the corrosion

resistance of steel, while the opposites suggested that the combined effects of galvanic coupling and internal acidification increase the corrosion rate of steel. For the formation mechanism of the corrosion scales on ferritic–pearlitic steels, it is suggested that the Fe<sub>3</sub>C in pearlite has a positive potential with respect to ferrite, which forms a galvanic couple between ferrite and Fe<sub>3</sub>C. Thus, the ferrite dissolves preferentially as an anodic phase and lamellar Fe<sub>3</sub>C in pearlite accumulates on the surface. However, there is lacking of direct proof about this suggestion, especially at the initial growth stage of corrosion scale. Therefore, it is great significant to clarify the formation mechanism of corrosion scale on the steel with ferritic–pearlitic microstructure.

In this work, the initial growth of the corrosion scale on low alloy steel with ferritic–pearlitic microstructure in carbon dioxide-saturated solution was studied by electrochemical impedance spectroscopy (EIS) measurements, and the morphologies of the corroded surface were also observed by scanning electron microscopy (SEM) after electrochemical measurements. It is anticipated that this study would provide the essential insight on the formation mechanism of corrosion scale of ferritic–pearlitic steel in CO<sub>2</sub>-containing environment.

## 2. Experimental

### 2.1. Materials and solutions

Low alloy steel, with a composition (mass%) of 0.16% C, 0.41% Si, 1.24% Mn, 0.019% P, 0.012% S, 0.02–0.15% V, 0.015–0.060% Nb,

\* Corresponding author. Tel.: +86 546 8393907; fax: +86 546 8393987.

E-mail address: [Dr.sunjianbo@gmail.com](mailto:Dr.sunjianbo@gmail.com) (J.B. Sun).

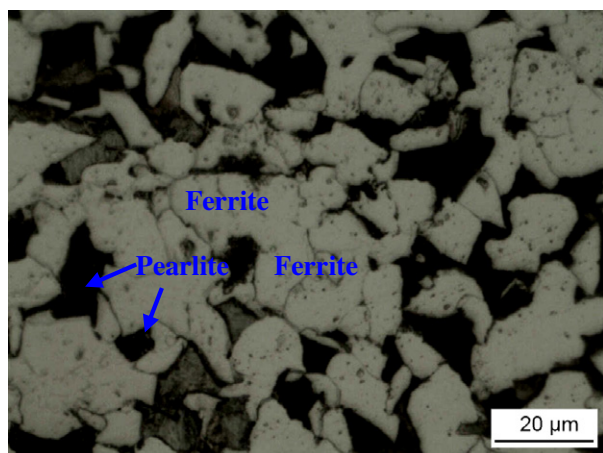


Fig. 1. Ferritic–pearlitic microstructure of low alloy steel.

0.02–0.20% Ti, and Fe balance, was used in this experiment. The microstructure of steel was composed of ferrite and pearlite after normalizing treatment, as shown in Fig. 1. Low alloy steel plate was machined into small pieces as working electrode (WE). Copper wire was welded to WE to ensure electrical contact for electrochemical measurements, and then WE was mounted in the holder with epoxy resin with an exposure area of  $1 \times 1 \text{ cm}^2$ . WE was ground up to 800 grit silicon carbide paper, rinsed with deionized water and degreased with acetone.

Test solution was made up from analytical grade reagents and deionized water simulating the formation water drawn out from oil and gas fields. Its chemical composition was listed in Table 1. The solution was deaerated by purging  $\text{CO}_2$  (99.95%) for 4 h prior to test. WE was then immersed into the solution while  $\text{CO}_2$  gas purging was maintained at a low flow rate to ensure entire saturation throughout test.

## 2.2. Electrochemical measurements

A PARSTAT® 2273 electrochemical test system was used for electrochemical measurements. A three-electrode electrochemical cell was used with a platinum plate as counter electrode and a saturated calomel electrode (SCE) as reference electrode. In order to form corrosion scale on WE surface under controlled conditions, the potentiostatic polarization was performed. After WE was immersed in the solution for 15–30 min to obtain a stable open circuit potential (OCP), an anodic polarization potential of 0.15 V vs. OCP was applied to WE for 20, 300 s, 0.25, 0.5, 1, 3, 7, 12, and 24 h, respectively. After each potentiostatic polarization, EIS were measured immediately at OCP with a sinusoidal potential excitation of 10 mV amplitude in the frequency range from 100 kHz to 10 mHz. The impedance data were fitted with Zview software using equivalent circuit.

All the tests were performed at ambient temperature and atmospheric pressure of  $\text{CO}_2$ .

## 2.3. Surface characterization

After electrochemical tests, electrodes were removed and rinsed with deionized water. The surface morphologies were analyzed by scanning electron microscope (SEM).

## 3. Results

### 3.1. EIS measurements after anodic polarization for various times

Fig. 2 shows the EIS of the electrodes after potentiostatic polarization for 20 and 300 s. It is seen that there is a similar feature of Nyquist plots in both electrodes, i.e. one depressed capacitive semicircle at high frequency and one inductive semicircle at low frequency. The capacitive semicircle at high frequency is attributed to the double layer capacitance and the charge transfer resistance, while the inductive semicircle at low frequency is related to the adsorbed intermediate product formed during the dissolution of electrode [22,23]. The corresponding Bode plots show that there are two time constants, i.e. a high-frequency peak and a low-frequency valley. The peak with a maximum phase angle decreases and shifts to low frequencies with the increase of anodic polarization time, which is usually associated with an increase of double layer capacitance with longer immersion time [24,25]. Furthermore, the diameter of the capacitive semicircle in Nyquist plots, i.e. the charge transfer resistance which represents the corrosion rate, after anodic polarization for 300 s is smaller than that after anodic polarization for 20 s. This indicates that the corrosion rate of electrode increases with anodic polarization time.

The EIS of the electrodes after anodic polarization for 0.25, 0.5, and 1 h are shown in Fig. 3. It is seen that in addition to the capacitive semicircle at high frequency and the inductive semicircle at low frequency observed in the EIS of electrodes after anodic polarization for 20 and 300 s, the third capacitive semicircle appears at lower frequency. It should be pointed out that only the initial part of the third capacitive semicircle is observed in Nyquist plot due to the insufficient low measured frequency. The appearance of this new capacitive semicircle is related to the formation of corrosion scale ( $\text{FeCO}_3$ ) on the electrode surface [22]. The corresponding Bode plots show three time constants corresponding to a high-frequency peak, a low-frequency valley and a low-frequency “semi-peak”. The Nyquist plots also show that the diameter of the capacitive semicircle decreases with the prolongation of polarization times, i.e. a higher corrosion rate of electrode after longer anodic polarization time. Meanwhile, a decrease of the diameter of low-frequency inductive semicircle is observed with the increase of polarization time, which is attributed to the decrease of adsorption area of intermediate reaction product ( $\text{FeOH}_{ad}$ ).

Fig. 4 shows the EIS of the electrode after anodic polarization for 3 h. It is seen that there are only a high-frequency capacitive semicircle and a low-frequency capacitive semicircle in the Nyquist plot. The low-frequency inductive semicircle has disappeared. The corresponding Bode plot shows two time constants, i.e. a high-frequency peak and a low-frequency “semi-peak”. For further prolongation of the anodic polarization times, EIS of electrodes after polarization for 7, 12, and 24 h are shown in Fig. 5. It is seen that the low frequency capacitive semicircle, which represents the formation of corrosion scale ( $\text{FeCO}_3$ ) on the electrode surface, switches to lower frequency, indicating a long relaxation process. The diameter of the capacitive semicircle also decreases with the prolongation of polarization times. The corresponding Bode plots also show that the peak with maximum phase angle decreases and shifts to low frequency with the increase of anodic polarization time, which is usually correlated to an increase of double layer capacitance with longer immersion time.

Table 1  
Concentration of formation water drawn out from oil fields.

Composition	$\text{K}^+ + \text{Na}^+$	$\text{Mg}^{2+}$	$\text{Ca}^{2+}$	$\text{Cl}^-$	$\text{SO}_4^{2-}$	$\text{HCO}_3^-$	Total ion concentration
Concentration (g/L)	7.032	0.012	0.694	11.451	0.455	0.403	20.047

Download English Version:

<https://daneshyari.com/en/article/1469628>

Download Persian Version:

<https://daneshyari.com/article/1469628>

[Daneshyari.com](https://daneshyari.com)